

# The infrared multiphoton excitation and photochemistry of DN<sub>3</sub>

T. B. Simpson, E. Mazur, K. K. Lehmann,<sup>a)</sup> I. Burak,<sup>b)</sup> and N. Bloembergen

Gordon McKay Laboratory, Harvard University, Cambridge, Massachusetts 02138  
(Received 6 December 1982; accepted 29 June 1983)

Multiphoton excitation and dissociation of DN<sub>3</sub> by short CO<sub>2</sub> laser pulses is shown to be a collisionless process. The characteristic features of this multiphoton process are systematically studied. The average number of photons absorbed per DN<sub>3</sub> molecule and the absolute dissociation yield show a strong dependence on the peak laser intensity. Resonantly enhanced coherent multiphoton excitation, rather than stepwise incoherent excitation, is suggested. The primary dissociation products of DN<sub>3</sub> are ND[<sup>1</sup>Δ] and N<sub>2</sub>. Formation of vibrationally excited ND[<sup>1</sup>Δ] intermediates is suggested. The reactions of ND[<sup>1</sup>Δ] with DN<sub>3</sub> lead to chemiluminescent signals originating from the formation of electronically excited ND<sub>2</sub>[<sup>2</sup>A<sub>1</sub>] and ND[<sup>3</sup>Π]. Formation of the ND[<sup>3</sup>Π] intermediate is attributed to a reaction of ND[<sup>1</sup>Δ] and vibrationally excited DN<sub>3</sub> molecules: ND[<sup>1</sup>Δ] + DN<sub>3</sub><sup>v</sup> → ND[<sup>3</sup>Π] + ND[<sup>3</sup>Σ<sup>-</sup>] + N<sub>2</sub>.

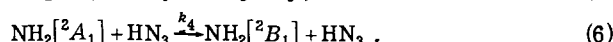
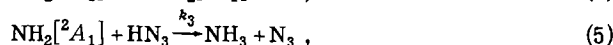
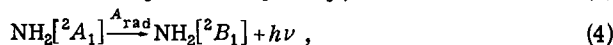
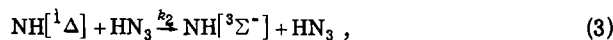
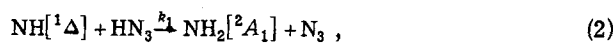
## I. INTRODUCTION

Since the first demonstration of collisionless infrared multiphoton excitation (IRMPE) of SF<sub>6</sub> in 1973 more than 100 molecular systems have been reported to undergo IRMPE or multiphoton dissociation (IRMPD) under the action of intense infrared laser radiation.<sup>1</sup> The generally accepted quasicontinuum model<sup>2</sup> of IRMPE requires a high density of vibrational states. In small polyatomics, the density of vibrational states grows so slowly with vibrational energy that the vibrational quasicontinuum can only be reached after significant excitation. Observation of IRMPE in triatomic or four atom molecules could therefore imply that a different mechanism is important.

IRMPE and IRMPD of three and four atom molecules have been reported by many authors. Some of the measurements were done at gas pressures of 1 Torr or higher using 100 ns laser pulses so that the excitation cannot be considered strictly collisionless. Several other experiments,<sup>3(a)-3(f)</sup> including work on deuterated hydrogen azide DN<sub>3</sub><sup>3(a)</sup> were done at lower pressures but did not conclusively show that dissociation resulted from collisionless excitation. No estimates of dissociation yield were made. The reported dissociation of carbonyl sulfide OCS,<sup>3(f)</sup> done under collisionless conditions, is inconsistent with more recent results.<sup>3(g)</sup> Finally, the interesting observation that in thiophosgene, Cl<sub>2</sub>CS, the efficiency of IRMPE decreases with increasing pressure,<sup>3(h)</sup> has not been shown to occur in other molecules.

In this paper a detailed and systematic study of the IRMPE and IRMPD of DN<sub>3</sub> is presented. The main objectives of the experiment were, first, to gain insight into the IRMPE process of DN<sub>3</sub> and second, to obtain information about the IR induced photochemistry of DN<sub>3</sub> and compare it with the UV induced photochemistry.

Before proceeding to the present experiment, a short recapitulation of the published analysis of the UV photochemistry of HN<sub>3</sub><sup>4,5</sup> is instructive as background to our analysis. After excitation at 266 nm, HN<sub>3</sub> was found to yield NH in the vibrationless <sup>1</sup>Δ electronic state as a primary dissociation product. The resulting photochemistry is described<sup>4</sup> by the following primary (1) and secondary (2)–(6) reactions:



The energy level diagram of the various states of NH is shown in Fig. 1. In process (2) the metastable NH[<sup>1</sup>Δ]

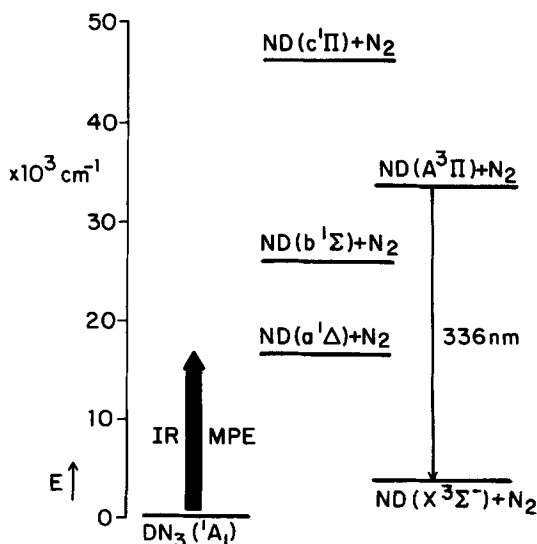


FIG. 1. Electronic energy level diagram of the dissociation products ND + N<sub>2</sub> of DN<sub>3</sub>.

<sup>a)</sup> Permanent address: Mallinckrodt Chemical Laboratory, Harvard University, Cambridge, MA 02138.

<sup>b)</sup> Permanent address: Institute of Chemistry, Tel Aviv University, Tel Aviv, Israel.

reacts with HN<sub>3</sub> to produce electronically excited NH<sub>2</sub>, which in turn radiatively relaxes producing a chemiluminescent signal. It was found that the quenching rate  $k_2$  is small compared to the reactive rate  $k_1$ . According to the kinetic scheme presented above, the transient behavior of this chemiluminescent signal should be characterized by exponential rise and fall times.

The vapors of DN<sub>3</sub> and HN<sub>3</sub> exhibit, respectively, a strong and a weak absorption band coinciding with the 10.6  $\mu\text{m}$  radiation of the CO<sub>2</sub> laser. The strong absorption band of DN<sub>3</sub>, centered at 954  $\text{cm}^{-1}$ , is associated with the DN bending fundamental  $\nu_4$ .<sup>6</sup> The HN<sub>3</sub> absorption band centered at 950  $\text{cm}^{-1}$  is a ( $\nu_2 - \nu_4$ ) hot band.<sup>6</sup> Hartford<sup>3(a)</sup> has reported the observation of a chemiluminescent emission from DN<sub>3</sub> and HN<sub>3</sub> vapors irradiated by intense CO<sub>2</sub> laser pulses. Most of his work focused on the kinetics of the DN<sub>3</sub> chemiluminescence. The results were analyzed in terms of a modified primary reaction (1):



and the secondary reactions (2)–(6) in which H is replaced by D. The rise and fall rates of the chemiluminescent signal can be expressed in terms of the rate constants in Eqs. (2)–(6) as

$$\alpha_{\text{rise}} = (k_3 + k_4)p + A_{\text{rad}}, \quad (7)$$

$$\alpha_{\text{fall}} = (k_1 + k_2)p. \quad (8)$$

Here,  $\alpha_{\text{rise}}$  and  $\alpha_{\text{fall}}$  are the reciprocal exponential rise and fall times of the chemiluminescent signal, respectively, and  $p$  is the pressure. The rise and fall times are determined by the rates of depletion of ND<sub>2</sub>[<sup>2</sup>A<sub>1</sub>] and ND[<sup>1</sup>Δ], respectively, see Eqs. (2), (3), (5), and (6).

## II. EXPERIMENTAL TECHNIQUE

The CO<sub>2</sub> laser used to pump the DN<sub>3</sub> has been described in detail in Refs. 7 and 8. Single mode 100 ns pulses are obtained from a hybrid TEA oscillator consisting of a Tachisto model 215 discharge head and a low pressure (4.5 Torr) discharge tube. Shorter, 30 ns pulses are produced by truncating the 100 ns pulses in a plasma shutter. Finally, 0.5 ns pulses are obtained through optical free induction decay of the truncated pulses. All of the pulses, 100, 30, or 0.5 ns are amplified by a series of Lumonics 103 and 280 TEA discharge units. Unless stated otherwise the oscillator was tuned to the P(18) line of the 10.6  $\mu\text{m}$  branch.

Samples of DN<sub>3</sub> are produced by mixing dried D<sub>3</sub>PO<sub>4</sub> with an excess of NaN<sub>3</sub>. Mass spectra showed that the gas produced contained no molecules of mass greater than 44 and that at least 70% was DN<sub>3</sub>. The CO<sub>2</sub> laser was focused into a cell containing the DN<sub>3</sub> by different combinations of mirrors and lenses to produce various beam waists. Beam sizes are measured by a scanning 50  $\mu\text{m}$  pinhole and pyroelectric detector. The CO<sub>2</sub> laser pulse energy is monitored by a second pyroelectric detector calibrated with a Scientech Joulemeter.

Optoacoustic measurements were carried out following the procedure described in Ref. 8. Brass baffles are placed in the cell in order to isolate the region

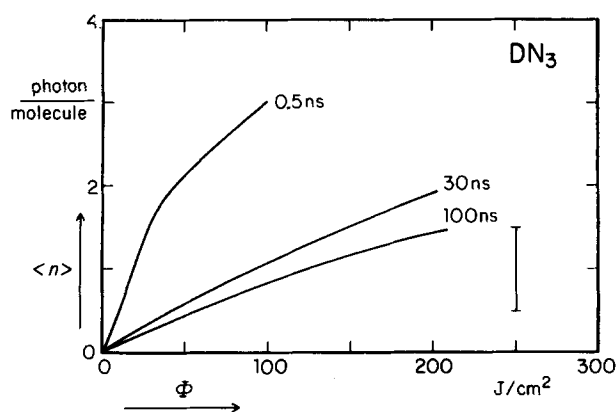


FIG. 2. The average number of photons absorbed per molecule ( $\langle n \rangle$ ) as a function of the CO<sub>2</sub> laser fluence  $\Phi$  for DN<sub>3</sub> at a pressure of 100 mTorr and room temperature. Each curve represents a smooth curve through approximately 100 data points with the scatter about the curves indicated by the error bar. The estimated error in absolute calibration of both axes is  $\pm 50\%$ . The laser was tuned to the P(18) line of the 10.6  $\mu\text{m}$  branch.

where the laser beam is collimated. A General Radio microphone is placed close to the focal volume. Luminescence resulting from IRMPD was measured by either a blue (EMI 9635 QB) or red sensitive (Hamamatsu R712) photomultiplier tube. Various Corning and Schott colored glass filters were used to isolate spectral regions. All signals were recorded by a home assembled data acquisition system based on the DEC LSI-11/2 microprocessor. Transient measurements were monitored and processed on a Biomation 8100 waveform digitizer and subsequently analyzed by computer.

## III. RESULTS

### A. Optoacoustic measurements

The optoacoustic signal of a 100 mTorr sample of DN<sub>3</sub> is plotted as a function of laser fluence for three different pulse lengths in Fig. 2. At 100 mTorr the average time between collisions is approximately 1  $\mu\text{s}$ , allowing an essentially collision-free excitation. The data show that the IRMPE of DN<sub>3</sub> is a strong function of peak laser intensity as well as laser fluence. The microphone signal has been calibrated to the average number of photons absorbed per molecule by means of a transmission measurement. The absolute calibration in Fig. 2 is accurate to  $\pm 50\%$ .

Tuning the laser to different lines in the 9.4 and 10.6  $\mu\text{m}$  CO<sub>2</sub> branches, it was observed that the IRMPE was confined to those lines that fall within the  $\nu_4$  small signal absorption band. These results are shown in Fig. 3. The relative microphone signal is plotted for the 0.5 ns pulses at a fluence of 20  $\text{J}/\text{cm}^2$ , and a pressure of 0.95 Torr. The peak of the IRMPE signal is near the central frequency 954  $\text{cm}^{-1}$  of the  $\nu_4$  band.

### B. IR induced chemiluminescence

The study of the IR induced chemiluminescence is carried out using a CO<sub>2</sub> laser beam focused to a waist

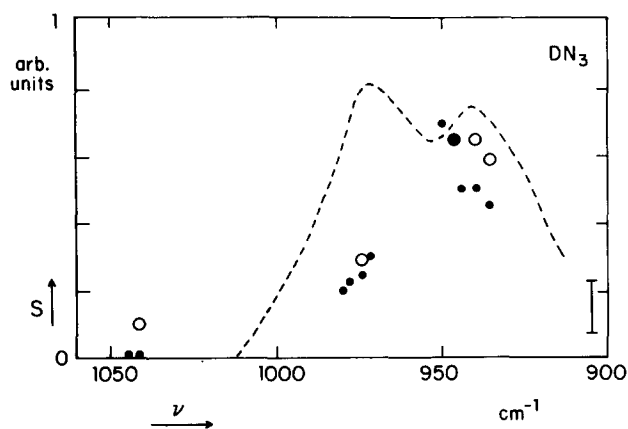


FIG. 3. Infrared absorption spectrum of DN<sub>3</sub>. ---: Low-resolution small signal IR absorption curve. ●: relative IR induced chemiluminescent signal at 20 mTorr, ○: relative IR induced optoacoustic signal at 950 mTorr. The laser induced signals were obtained with 0.5 ns pulses.

of 0.02 cm, collimated over a length of 1 cm. The collimated region is viewed by a photomultiplier which monitors the induced chemiluminescence. The tight focusing serves to increase the CO<sub>2</sub> laser fluence up to values of 150 J/cm<sup>2</sup> for the 0.5 ns pulses, and secondly, to minimize the reaction of the primary dissociation product ND with vibrationally excited DN<sub>3</sub> molecules. With the present geometry the mean free path of the molecules at a pressure of 200 mTorr is of the same order of magnitude as the beam diameter. At lower pressures the reactions of ND with cold DN<sub>3</sub> molecules is expected to be dominant.

Figure 4 shows the luminescence spectrum obtained with a 0.5 ns pulse of 30 J/cm<sup>2</sup>. The visible spectrum has been obtained by observing the chemiluminescence through various optical and interference filters. The emission extends from about 400 nm to the cutoff of the photomultiplier between 800–900 nm. The relative magnitude of the spectrum was independent of the laser fluence at pressures below 100 mTorr. Essentially the

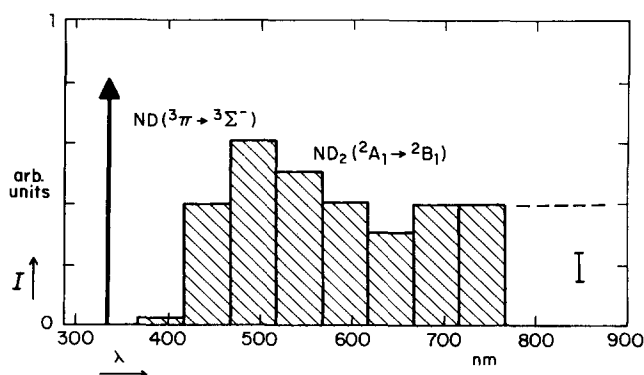


FIG. 4. Chemiluminescence spectrum of DN<sub>3</sub>. The bars represent the relative intensity of various spectral regions obtained by changing the short wavelength cutoff of long pass filters. The data was obtained at 15 mTorr with 0.5 ns pulses of 30 J/cm<sup>2</sup>.

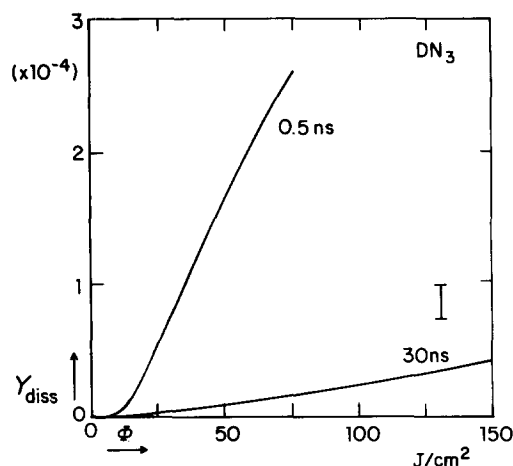


FIG. 5. Fluence dependence of the visible chemiluminescent signal for two pulse durations. Each curve represents a smooth curve through approximately 100 data points with the scatter about the curves indicated by the error bar. The vertical scale has been calibrated to the dissociation yield (see the text).

same relative visible luminescence spectra were obtained for the 30 ns pulses. This emission is attributed to the <sup>2</sup>A<sub>1</sub> → <sup>2</sup>B<sub>1</sub> transition of ND<sub>2</sub> in accordance with Ref. 3. The other spectral feature in Fig. 4 is a sharp UV emission. Using a monochromator with 1 nm resolution, this emission was identified as the <sup>3</sup>Π → <sup>3</sup>Σ<sup>+</sup>Q-branch transition of ND at 336 nm.<sup>9</sup>

Figure 5 displays the fluence dependence of the visible chemiluminescent signal for 0.5 and 30 ns pulses. It should be mentioned that the same fluence dependence was found for separate spectral regions of the signal. The signal for the 0.5 ns pulses is an order of magnitude larger than the ones for the 30 ns pulses. The time integrated intensity of the chemiluminescent signal can be related to the absolute dissociation yield  $Y_{diss}$ . If one assumes that all the ND molecules form ND<sub>2</sub>[<sup>2</sup>A<sub>1</sub>] molecules as in Eq. (2), calibration of the vertical scale is achieved as follows. First the number of photons emitted is estimated from the (time integrated intensity of the) chemiluminescent signal, taking into account the characteristics of and the solid angle viewed by the photomultiplier. This number is connected to the number of ND<sub>2</sub>[<sup>2</sup>A<sub>1</sub>] molecules (which under the above assumption is equal to the number of dissociated DN<sub>3</sub> molecules) using the fluorescence yield of the ND[<sup>2</sup>A<sub>1</sub>] molecules, see Eq. (10). The dissociation yield  $Y_{diss}$ , i.e., the fraction of dissociated DN<sub>3</sub> molecules, is finally obtained by dividing the number of ND<sub>2</sub>[<sup>2</sup>A<sub>1</sub>] molecules by the total number of DN<sub>3</sub> molecules in the focal volume of the laser beam. An independent calibration, using a quadrupled Nd:YAG laser at 266 nm and the absorption data of Ref. 4, yielded the same results. This second calibration is independent of the branching yields for ND[<sup>1</sup>A] showing that indeed a large fraction of ND[<sup>1</sup>A] forms ND<sub>2</sub>[<sup>2</sup>A<sub>1</sub>]. We caution, however, that this calibration and the vertical scale in Fig. 5 should only be considered as an order of magnitude estimate of the dissociation yield and not as a precise determination.

Comparing Fig. 5 to Fig. 2 it is immediately evident

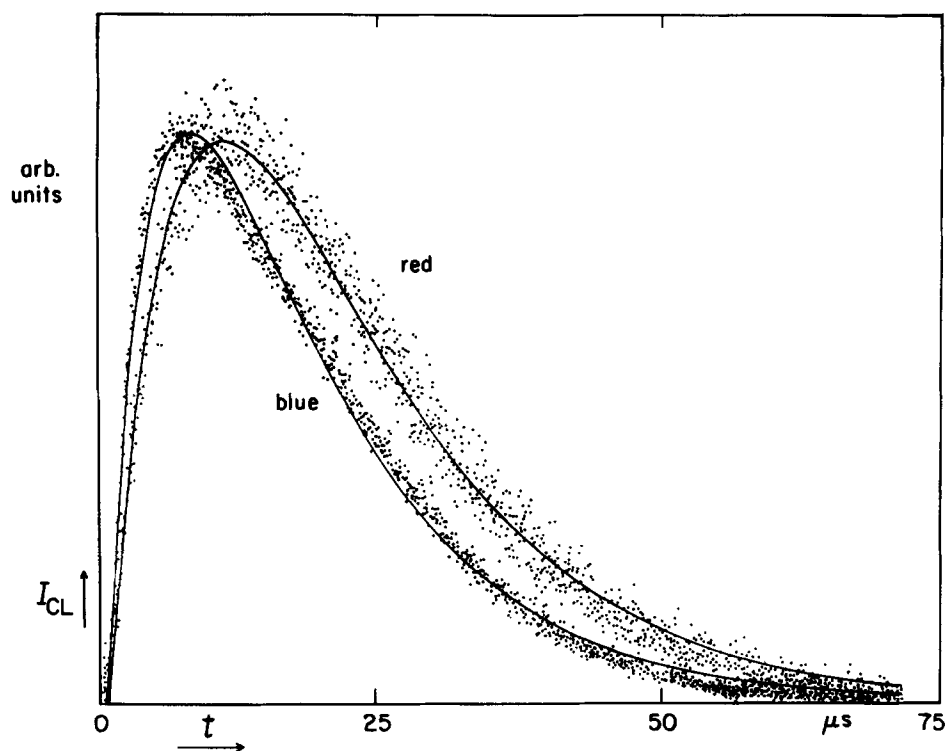


FIG. 6. Transient behavior of the IR induced visible chemiluminescence of  $\text{DN}_3$  at 29 mTorr in two spectral regions: blue (400–500 nm) and red (600–800 nm). The traces are obtained with 0.5 ns pulses at approximately  $75 \text{ J/cm}^2$ . Curves with exponential rise (5 and  $8 \mu\text{s}$ , respectively) and fall (13 and  $14 \mu\text{s}$ , respectively) are fitted to the data points.

that dissociation of  $\text{DN}_3$  occurs even at fluences where the average absorption is at most a few photons, well below the  $18 \pm 1$  photons required for dissociation as in Eq. (1a). The visible luminescence signal for various  $\text{CO}_2$  laser lines is plotted in Fig. 3. As with the opto-acoustic measurements, all lines giving significant excitation fall within the  $\nu_4$  absorption band.

The time dependent behavior of the visible luminescence in two spectral regions, blue (400–500 nm) and red (600–800 nm) is shown in Fig. 6. The data are analyzed by a least square fit of a curve with exponential rise and fall times. Within experimental error, the two sets of data points share a common fall time of  $13 (\pm 1) \mu\text{s}$ . However, the rise time of the blue emission is  $5 \mu\text{s}$ , while the rise time of the red chemiluminescence is about  $8 \mu\text{s}$ . The pressure dependence of the rise and fall times for the red signals agree very well with the results obtained by Hartford.<sup>3</sup>

A verification of the collisionless character of the MPD process is provided by a study of the pressure dependence of the time integrated chemiluminescent signal. If the MPE process is indeed collisionless, the total number of  $\text{ND}[^1\Delta]$  intermediates is proportional to the pressure  $p$ . If these intermediates are moreover scavenged by process (2), the number of electronically excited  $\text{ND}_2[^2A_1]$  intermediates is also proportional to  $p$ , i.e.,

$$N_{\text{ND}_2} = \alpha(\phi)p, \quad (9)$$

with  $\alpha(\phi)$  a proportionality factor depending on the laser fluence,  $\phi$ . The yield of fluorescence from  $\text{ND}_2[^2A_1]$ , on the other hand, is given by

$$Y = \frac{A_{\text{rad}}}{A_{\text{rad}} + (k_3 + k_4)p}. \quad (10)$$

The pressure dependence of the time integrated intensity of the chemiluminescent signal  $I_{\text{sig}}$  can now be obtained from

$$I_{\text{sig}} = N_{\text{ND}_2} Y. \quad (11)$$

Inverting this equation and substituting Eqs. (9) and (10) one obtains

$$I_{\text{sig}}^{-1} = \alpha^{-1}(\phi) \left[ \frac{k_3 + k_4}{A_{\text{rad}}} + p^{-1} \right], \quad (12)$$

which shows that collisionless dissociation of  $\text{DN}_3$  requires a linear relation between  $I_{\text{sig}}^{-1}$  and  $p^{-1}$ . The experimental results shown in Figs. 7(a) and 7(b) corresponding to the red and blue chemiluminescence, respectively, indeed obey this linear behavior. At pressures above 100 mTorr the blue signals [see Fig. 7(b)] show deviations from linearity, which is attributed to "hot" reactions between  $\text{ND}[^1\Delta]$  and vibrationally excited  $\text{DN}_3$  molecules. Using the experimentally determined value of  $k_3 + k_4 = 3.4 \times 10^6 \text{ s}^{-1} \text{ Torr}^{-1}$ ,<sup>3</sup> radiative lifetimes of  $12 \pm 2$  and  $5 \pm 1 \mu\text{s}$  of  $\text{ND}_2[^2A_1]$  are obtained for the red and blue emission, respectively. For comparison, the characteristic lifetimes of  $\text{NH}_2[^2A_1]$ , obtained by optical excitation of  $\text{NH}_2[^2B_1]$  at wavelength around  $600 \mu\text{m}$ , are on the order of  $10 \mu\text{s}$ .<sup>10</sup>

### C. UV luminescence

The narrow band UV luminescence at 336 nm originates from the  $^3\Pi - ^3\Sigma^-$  transition of ND. The temporal characteristics of this luminescence show a dependence on beam geometry and gas pressure. At pressures be-

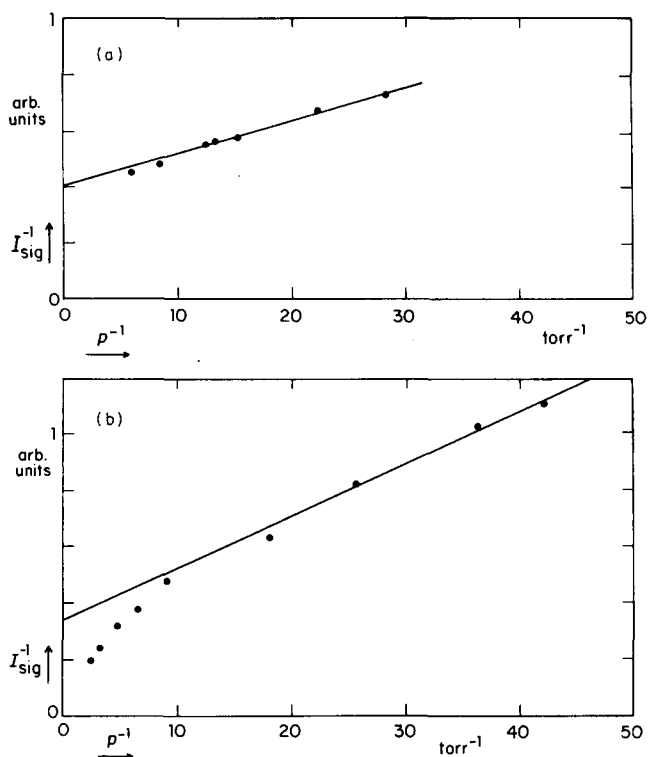


FIG. 7. Pressure dependence of the IR induced visible chemiluminescence of  $\text{DN}_3$ . (a) in the red (600–800 nm) and (b) in the blue (400–500 nm). The lines are a least square fit according to Eq. (12).

low 150 mTorr, the risetime depends on the beam geometry and is independent of pressure, while the fall time depends only on the gas pressure. A typical time trace of the signal at a pressure of 40 mTorr and laser

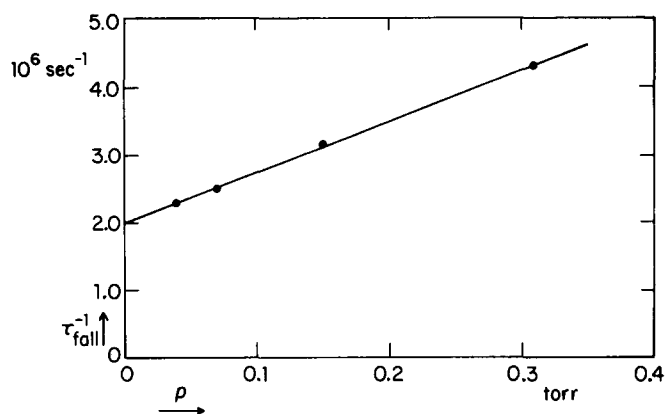


FIG. 9. Reciprocal fall times of the UV chemiluminescence of  $\text{DN}_3$  as a function of pressure. The points were obtained with 0.5 ns pulses.

beam waist of 0.02 cm is shown in Fig. 8. The rise and fall times, found to be 57 and 425 ns, are much shorter than the ones for the visible chemiluminescent signal. Changing the beam waist from 0.01 to 0.04 cm causes the risetime to increase from roughly 40 to 120 ns. A Stern-Volmer plot of the fall rates is shown in Fig. 9, yielding a collision quenching rate of  $7.5 \times 10^6 \text{ s}^{-1} \text{ Torr}^{-1}$  and an intercept corresponding to  $(0.5 \pm 0.05 \mu\text{s})^{-1}$ . This intercept should be compared with the reported life times of the  $\text{NH}[\text{}^3\Pi]$  state, which are on the order of 450 ns.<sup>11,12</sup>

At intermediate pressures ( $0.15 \text{ Torr} \lesssim p \lesssim 3 \text{ Torr}$ ) the fall of the signal no longer follows a simple exponential dependence and becomes relatively insensitive to pressure. The fall time of the signal decreases by less than a factor of 2 over the pressure range from

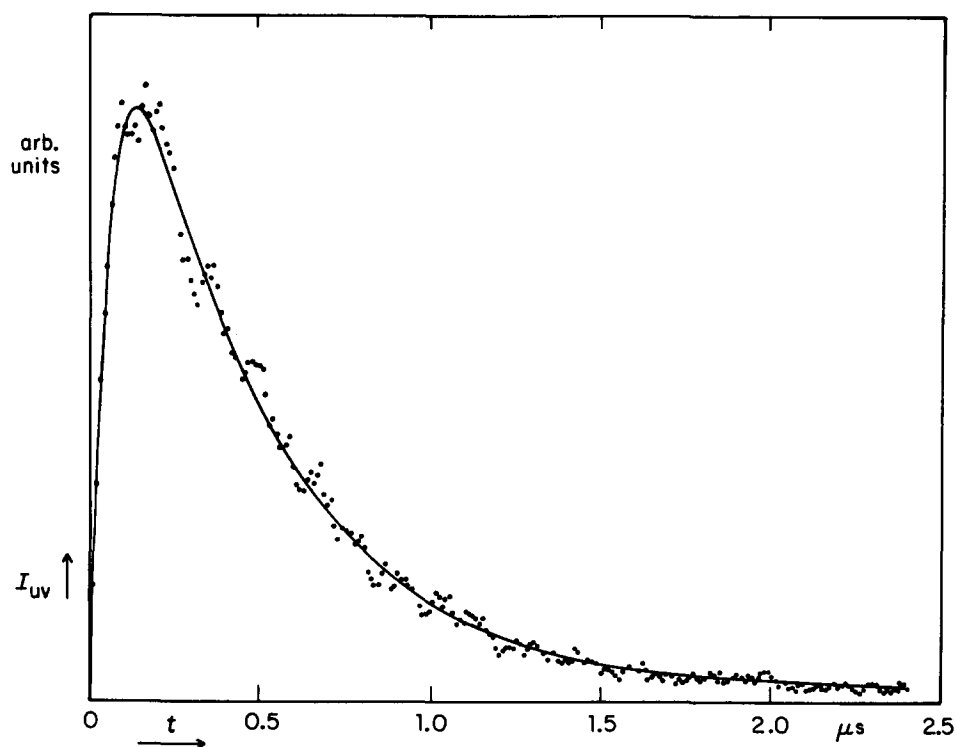


FIG. 8. Transient behavior of the IR induced UV chemiluminescence of  $\text{DN}_3$  at 40 mTorr. The trace was obtained with 0.5 ns pulses. A curve with exponential rise and fall times (0.06 and 0.43  $\mu\text{s}$ , respectively) is fitted to the data points.

0.25 to 3 Torr. The onset of this intermediate pressure behavior depends on the laser beam waist; the larger the waist, the lower the pressure where the fall time deviates from simple exponential behavior. At pressures above 3 Torr both the luminescence rise and fall times decrease with increasing pressure.

The time integrated UV signal was measured as a function of pressure and laser fluence. It appeared to be proportional to the square of the pressure, see Fig. 10, indicating that  $\text{ND}[^3\Pi]$  is not a primary dissociation product but rather a result of collisions of excited species. It should be pointed out here that the number of  $\text{ND}[^3\Pi]$  molecules is small compared to the number of primary dissociation products, i.e., the  $\text{ND}[^1\Delta]$  molecules. Comparing the UV and visible chemiluminescence and taking into account the quenching rates of  $\text{ND}_2[^2A_1]$  and  $\text{ND}[^3\Pi]$  the number ratio of  $^3\Pi$  to  $^1\Delta$  for ND is estimated to be  $10^{-3}$  (for 0.5 ns pulses at a fluence of  $150 \text{ J/cm}^2$  and a pressure of 20 mTorr).

The dependence of the integrated UV signal on fluence is stronger than that of the visible chemiluminescence. From the logarithmic slope in Fig. 11 the following relation between the UV and the visible signal  $I_{UV}$  and  $I_{vis}$ , respectively, can be deduced:

$$I_{UV} \propto (I_{vis})^{1.8}. \quad (13)$$

For the 30 ns pulses the signal to noise ratio was too small to give significant results.

The temporal behavior of the UV emission changes drastically when a buffer gas is added. Figure 12 shows the transient UV signal as well as the visible chemiluminescent signal for a  $\text{DN}_3$ -Ar mixture. It is to be noted that the UV emission has much longer rise and fall times than in the case of pure  $\text{DN}_3$ . The  $3.9 \mu\text{s}$  fall time of the UV signal is very close to the  $4.5 \mu\text{s}$  fall time of the visible emission. A detailed discussion of these observations follows in the next section.

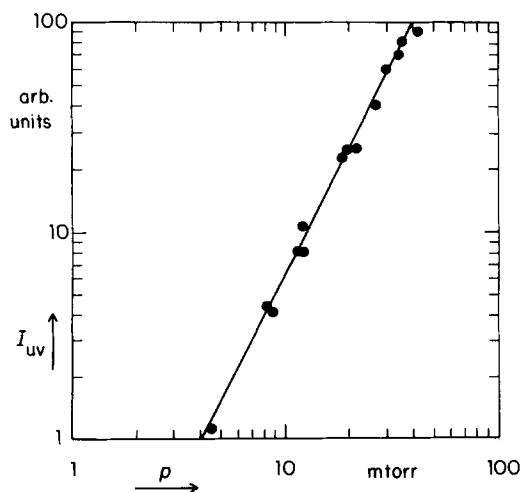


FIG. 10. The integrated intensity of the UV signal as a function of pressure of  $\text{DN}_3$  plotted double logarithmically. The slope of the line is 2.

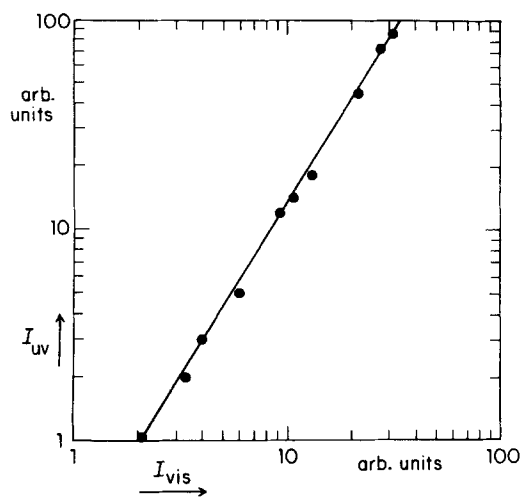


FIG. 11. Ultraviolet vs visible chemiluminescence signal for  $\text{DN}_3$  plotted double logarithmically. Each point corresponds to a certain fluence.

#### D. IRMPE of $\text{HN}_3$

Signals obtained from similar experiments on  $\text{HN}_3$  were at least an order of magnitude smaller. Therefore, a detailed study of the IRMPE characteristics of  $\text{HN}_3$  could not be performed. We established, however, that IR multiphoton excitation of  $\text{HN}_3$ , just as  $\text{DN}_3$ , yields a UV emission at 336 nm and a broad visible chemiluminescence.

### IV. DISCUSSION

#### A. Mechanism of infrared multiphoton excitation of $\text{DN}_3$

The experiments presented in this paper confirm that infrared multiphoton dissociation of  $\text{DN}_3$  can be achieved without collisions [see Fig. 7, cf. Eq. (12)]. In contrast to larger molecules the IRMPD of  $\text{DN}_3$  cannot proceed through the incoherent excitation mechanism of the quasicontinuum model.<sup>2</sup> This model requires that the spacing of accessible energy levels is smaller than the bandwidth of the laser pulse, in our case  $10^{-2}$  and  $10^{-3} \text{ cm}^{-1}$  for 0.5 and 30 ns pulses, respectively. A Whitten-Rabinovitch estimate of the density of vibrational states,<sup>13</sup> plotted in Fig. 13, is even at the dissociation limit an order of magnitude too small to satisfy this condition. The density of accessible states could be significantly larger if rotational as well as vibrational selection rules break down. Even so, there will still be an energy range of several thousand wave numbers with insufficient density of states for resonant stepwise excitation.

The multiphoton dissociation of  $\text{DN}_3$  shows a strong dependence on pulse duration and, hence, on intensity. There is an order of magnitude difference between the two curves in Fig. 5, whereas for large molecules such as  $\text{SF}_6$  only small differences have been observed.<sup>14</sup> Furthermore, from the data in Fig. 5 it follows that  $Y_{\text{diss}}$  is proportional to the fluence  $\Phi$  raised to the power  $2 \pm 0.5$  and not 18 as would be the case if the IRMPD of

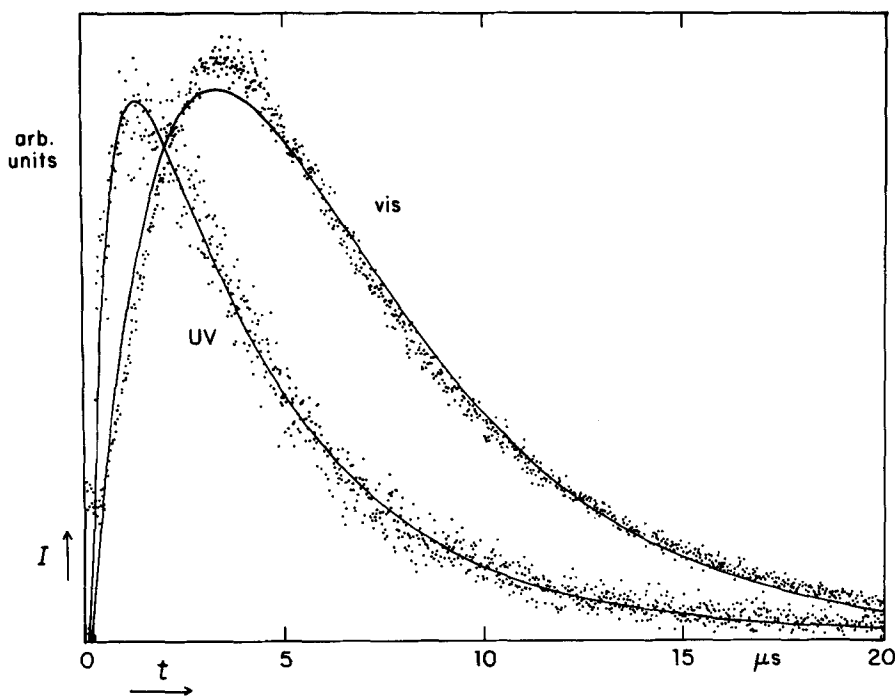


FIG. 12. Transient behavior of IR induced visible and UV chemiluminescence of 25 mTorr DN<sub>3</sub> in 9 Torr of Ar. The traces are obtained with 0.5 ns pulses. Curves with exponential rise (0.5 and 2.4  $\mu$ s, respectively) and fall (3.9 and 4.4  $\mu$ s, respectively) are fitted to the data points.

DN<sub>3</sub> resulted from the simultaneous absorption of 18 photons in the limit of weak field perturbation theory. At the extremely high intensities used in this experiment, the interaction energy  $\epsilon = \mu E$  of the electric field  $E$  with the molecules having a transition dipole moment  $\mu$ , is very large. For an intensity of  $10^{11}$  W/cm<sup>2</sup>, corresponding to a 0.5 ns pulse of 50 J/cm<sup>2</sup>, one has  $\epsilon \approx 10^2$   $\mu$  cm<sup>-1</sup>, with the unknown transition moment  $\mu$  in D. A transition moment of 0.1 D, reasonable for such a transition, at low excitation could already result in a dynamic Stark broadening of the intermediate states comparable to the Whitten-Rabinovitch estimate of the spacing of states. Consequently a resonantly enhanced multiphoton excitation to high vibrational states becomes possible.

### B. Photochemistry

In the previous section the visible chemiluminescence is attributed to the  ${}^2A_1 - {}^2B_1$  transition of ND<sub>2</sub>. The only possibility for the formation of electronically excited ND<sub>2</sub> is a reaction between DN<sub>3</sub> and ND as shown in Eq. (2). Other possibilities can be ruled out as follows. A reaction between two vibrationally excited DN<sub>3</sub> molecules yielding ND<sub>2</sub>[ ${}^2A_1$ ] would imply a  $p^2$  dependence of the chemiluminescence rather than the pressure dependence derived in Eq. (12). Furthermore in contradiction to the long duration of the chemiluminescent signal, these reactions would be restricted to short times after the excitation, since diffusion and vibrational relaxation rapidly diminish the probability of these events. Another possibility of formation of ND<sub>2</sub> is a reaction of vibrationally hot DN<sub>3</sub> with cold DN<sub>3</sub>. This mechanism can also be excluded since the observed fall time of the chemiluminescence is much larger than vibrational cooling of DN<sub>3</sub> by V-V transfer. The fact that the time evolution of the chemiluminescence is similar to the

one obtained by UV photolysis in HN<sub>3</sub><sup>4</sup> supports the formation of ND<sub>2</sub> according to reaction (2) as has been mentioned in the beginning. The pressure dependence of the chemiluminescence moreover shows that the formation of ND stems from collisionless multiphoton dissociation of DN<sub>3</sub>, as in Eq. (1a).

The formation of ND in various electronic states ( ${}^3\Sigma^-$ ,  ${}^1\Delta$ ,  ${}^1\Sigma^+$ ) has to be considered. A visible dye laser tuned to the ND[ $c\ {}^1\Pi - b\ {}^1\Sigma^+$ ] transition yielded no detectable laser induced fluorescence signal at the  ${}^1\Pi - {}^1\Delta$  transition in the UV showing that the formation of ND[ ${}^1\Sigma^+$ ] is insignificant. The ND[ ${}^1\Delta$ ] and ND[ ${}^3\Sigma^-$ ] could not be monitored because the relevant transitions  $c\ {}^1\Pi - a\ {}^1\Delta$  and  $A\ {}^3\Pi - X\ {}^3\Sigma^-$ , respectively, are not accessible to our dye laser. It is however, highly de-

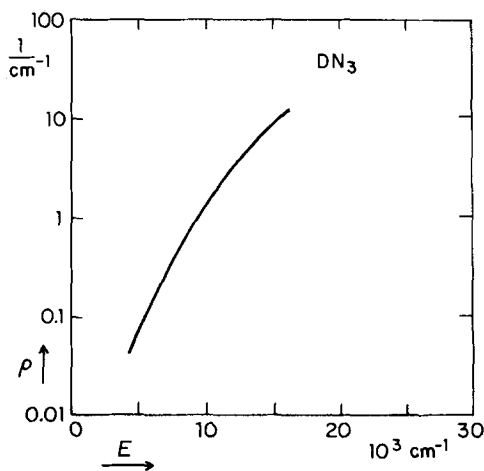
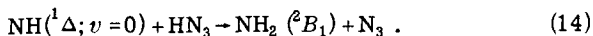


FIG. 13. Density of vibrational states of DN<sub>3</sub> vs vibrational energy  $E$ , as calculated from the Whitten-Rabinovitch formula.

sirable to perform such experiments in order to determine with certainty the state distributions of the primary dissociation products.

In shock-wave tube decomposition<sup>15,16</sup> and CO<sub>2</sub> laser initiated explosion<sup>17</sup> of HN<sub>3</sub>, the formation of both NH[<sup>1</sup>Δ] and NH[<sup>3</sup>Σ<sup>-</sup>] has been observed. Kajimoto *et al.* conclude that NH[<sup>3</sup>Σ<sup>-</sup>] is produced with an activation energy of 1.5 eV,<sup>16</sup> but in the explosion experiment the appearance of the <sup>3</sup>Σ<sup>-</sup> state starts only after 30 μs, suggesting that it is not a primary dissociation product. Moreover, it was shown that NH[<sup>3</sup>Σ<sup>-</sup>] does not react significantly with HN<sub>3</sub>.<sup>16</sup> For this reason the visible chemiluminescence observed in the IRMPE experiments presented here is attributed to a reaction of ND[<sup>1</sup>Δ] with DN<sub>3</sub>. Although formation of ND[<sup>3</sup>Σ<sup>-</sup>] is spin forbidden it cannot be totally ruled out.

An interesting feature of the IR induced chemiluminescence is that it is blue shifted with respect to the chemiluminescence observed in UV photolysis.<sup>4</sup> In the latter experiment it is shown that the short-wavelength cutoff at 600 nm corresponds very well with the 2.2 eV released by the reaction<sup>18,19</sup>

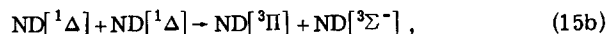


The shift of approximately 8000 cm<sup>-1</sup> (~1 eV) of the IR induced chemiluminescence can be attributed to the formation of vibrationally excited ND[<sup>1</sup>Δ]. Since DN<sub>3</sub> has six vibrational degrees of freedom, only a fraction of the excess energy above the dissociation limit is expected to go into the ND vibration. The presence of ND[<sup>1</sup>Δ] molecules with 1 eV or more of vibrational energy implies excitation of DN<sub>3</sub> far above the dissociation limit. This observation is hard to explain on the basis of a competition between the up-pumping rate and the RRKM dissociation rate. The RRKM rate 2 × 10<sup>9</sup> s<sup>-1</sup> at the dissociation limit, is calculated from the density of states in Fig. 13, assuming there is no barrier to the spin allowed dissociation channel.<sup>20</sup> Since the up-pumping rate changes with intensity, one expects the ratio of blue to red fluorescence to be intensity dependent. This ratio has been found, however, to be independent of both laser fluence and pulse duration, and hence of laser intensity.

An interesting speculation is the existence of a dynamical barrier, due to incomplete mixing of the normal mode vibrational states. Recent measurements of the overtone spectra of HN<sub>3</sub>, show that up to the dissociation limit very little mixing of the overtone states with the dense manifold of states occurs.<sup>21</sup> Classical trajectory calculations for C<sub>2</sub>H molecules above the dissociation limit<sup>22</sup> show, moreover, that large regions of the phase space do not lead to dissociation. Quantum states localized in these regions can only end up in the dissociative regions of phase space by tunneling through a "dynamical" barrier.

Collisional formation of highly excited ND[<sup>3</sup>Π] intermediates is demonstrated by the *p*<sup>2</sup> dependence of the UV emission at low pressures. Further, it apparently results from a collision between two reaction products.

This follows from the fact that the UV signal grows approximately as the square of the visible signal. Two spin allowed reactions could account for the formation of ND[<sup>3</sup>Π]:



where DN<sub>3</sub><sup>\*</sup> is highly vibrationally excited DN<sub>3</sub>. Both reactions are endothermic and require that the ND[<sup>1</sup>Δ] molecules have significant internal energy.

An important factor in the time evolution of the UV signal is the small volume initially occupied by the ND[<sup>1</sup>Δ] and DN<sub>3</sub><sup>\*</sup>. At low pressure the mean free path of the molecules exceeds the laser beam diameter. While the fall time is determined by the radiative and collisional lifetime of the ND[<sup>3</sup>Π], the risetime of the emission is completely determined by gas-kinetic and geometrical parameters. This is shown by the dependence of the risetime on beam geometry. As the ND[<sup>1</sup>Δ] and the DN<sub>3</sub><sup>\*</sup> diffuse out of the focal region the probability of reactions (15a) or (15b) decreases. Therefore, we may use a simplified (reversible) model for the diffusion to estimate this probability. Assuming cylindrical symmetry around the laser beam and an average radial velocity ⟨*v*⟩ of the molecules, the time evolution of the probability is given by

$$\frac{P(t)}{P(0)} = \left( \frac{r}{r + \langle v \rangle t} \right)^2, \quad (16)$$

with *r* the radius of the initial excitation zone. For ⟨*v*⟩ = 10<sup>5</sup> cm/s and *r* = 0.005 cm in 50 ns the probability decreases by a factor of 4 in good agreement with the observations.

The situation changes at high pressure. This is most dramatically shown by the addition of a buffer gas which confines the ND[<sup>1</sup>Δ] and DN<sub>3</sub><sup>\*</sup> to the excitation volume. The risetime of the UV emission is then essentially determined by the 0.5 μs lifetime of ND[<sup>3</sup>Π]. The fall time, determined by the lifetime of the reactants that form ND[<sup>3</sup>Π], is now almost equal to the fall time of the visible chemiluminescence. This is strong evidence that the formation of ND[<sup>3</sup>Π] is due to reaction (15a) and not to a collision between two ND[<sup>1</sup>Δ] molecules since the latter process, proportional to the ND[<sup>1</sup>Δ] concentration squared, would result in a fall time of the UV signal twice as short the one of the visible signal. The reaction shown in Eq. (15a) is very endothermic: an energy of 2.7 eV must be supplied by DN<sub>3</sub> and ND[<sup>1</sup>Δ] in the form of internal vibrational energy. This exceeds by 0.6 eV the dissociation threshold, which confirms the earlier assumption that highly excited DN<sub>3</sub> and ND molecules are formed in the excitation zone.

Apart from the more specific photochemistry, the present work shows the infrared multiphoton excitation characteristics for a small molecule. It is important to emphasize the difference in behavior with the by now well understood behavior for larger molecules. The nonstatistical aspects make DN<sub>3</sub> a particularly interesting system for further study.

## ACKNOWLEDGMENTS

This work was sponsored by the Army Research Office under Contract DAAG-29-81-K-0071. Eric Mazur would like to thank Dr. H. Schröder for a helpful discussion. The authors also would like to thank Dr. J. Tsao for advice concerning the experimental setup.

<sup>1</sup>For a recent review see: W. Fuss and K. L. Kompa, *Prog. Quantum Electron.* **7**, 117 (1981).

<sup>2</sup>N. Bloembergen and E. Yablonovitch, *Phys. Today* **31**, 23 (1978).

<sup>3</sup>This is a partial list of the work in the literature on IRMPE in small molecules, with at least one work on each molecule studied. For a more complete list see Ref. 1. (a) A. Hartford, Jr., *Chem. Phys. Lett.* **57**, 352 (1978); (b) G. Koren, M. Okon, and V. P. Oppenheim, *Opt. Commun.* **22**, 351 (1977); (c) J. W. Hudgens, J. L. Durant, Jr., D. J. Bogan, and R. L. Coveleskie, *J. Chem. Phys.* **70**, 5906 (1979); (d) R. V. Ambartsumyan, V. S. Dolzhikov, V. S. Letokhov, E. A. Ryabov, and N. V. Chekalin, *Sov. Phys. -JETP* **42**, 36 (1976); (e) J. D. Campbell, G. Hancock, J. B. Halpern, and K. H. Welge, *Chem. Phys. Lett.* **44**, 404 (1976); (f) D. Proch and H. Schröder, *ibid.* **61**, 426 (1979); (g) T. B. Simpson and N. Bloembergen, *Opt. Commun.* **37**, 256 (1981); (h) D. M. Brenner, M. N. Spencer, and J. I. Steinfeld, *J. Chem. Phys.* **78**, 137 (1983).

<sup>4</sup>A. P. Baronavski, R. G. Miller, and J. R. McDonald, *Chem. Phys.* **30**, 119 (1978).

<sup>5</sup>J. R. McDonald, R. G. Miller, and A. P. Baronavski, *Chem. Phys.* **30**, 133 (1978).

<sup>6</sup>D. Dows and G. C. Pimentel, *J. Chem. Phys.* **23**, 1258 (1955).

<sup>7</sup>H. S. Kwok and E. Yablonovitch, *Rev. Sci. Instrum.* **46**, 814 (1975).

<sup>8</sup>J. G. Black, P. Kolodner, M. J. Shultz, E. Yablonovitch, and N. Bloembergen, *Phys. Rev. A* **19**, 704 (1979).

<sup>9</sup>P. Bollmark, I. Kopp, and B. Rydh, *J. Mol. Spectrosc.* **34**, 487 (1970).

<sup>10</sup>J. B. Halpern, G. Hancock, M. Lenzi, and K. H. Welge, *J. Chem. Phys.* **63**, 4808 (1975).

<sup>11</sup>E. H. Fink and K. H. Welge, *J. Chem. Phys.* **46**, 4315 (1967).

<sup>12</sup>W. M. Smith, J. Brozowski, and P. Ermans, *J. Chem. Phys.* **64**, 4628 (1976).

<sup>13</sup>G. Z. Whitten and B. S. Rabinovitch, *J. Chem. Phys.* **38**, 2466 (1963).

<sup>14</sup>P. R. Kolodner, C. Winterfeld, and E. Yablonovitch, *Opt. Commun.* **20**, 119 (1977).

<sup>15</sup>I. S. Zaslanko, S. M. Kogarko, and E. V. Mozzhukhin, *Kinet. Katal.* **13**, 829 (1972).

<sup>16</sup>O. Kajimoto, T. Yamamoto, and T. Fueno, *J. Phys. Chem.* **83**, 429 (1979).

<sup>17</sup>P. Avouris, D. S. Bethune, J. R. Lankard, J. A. Ors, and P. Sorokin, *J. Chem. Phys.* **74**, 2304 (1981).

<sup>18</sup>H. Okabe, *J. Chem. Phys.* **49**, 2726 (1968).

<sup>19</sup>H. Okabe and M. Lenzi, *J. Chem. Phys.* **47**, 5241 (1967).

<sup>20</sup>A. Sevin, J. P. Le Roux, B. Bigot, and A. Devaquet, *Chem. Phys.* **45**, 305 (1980).

<sup>21</sup>K. K. Lehmann, G. J. Scherer, and W. Klemperer (to be published).

<sup>22</sup>R. J. Wolf and W. L. Hase, *J. Chem. Phys.* **72**, 316 (1980); **73**, 3779 (1980).